

Affinity and Mobility of Polyclonal Anti-Dansyl Antibodies Sequestered within Sol–Gel-Derived Biogels

Meagan A. Doody, Gary A. Baker, Siddharth Pandey, and Frank V. Bright*

Department of Chemistry, Natural Sciences Complex, University at Buffalo,
The State University of New York, Buffalo, New York 14260-3000

Received December 16, 1999. Revised Manuscript Received February 17, 2000

We report on the equilibrium binding affinity and rotational reorientation dynamics of intact polyclonal anti-dansyl antibodies (anti-DAN) sequestered within sol–gel-derived biogels. Our results show that the nanosecond rotational motions that are intrinsic to immunoglobulin G antibodies when they are dissolved in aqueous buffer are arrested in an aged biogel. However, even though the anti-DAN rotational mobility is not detectable in a biogel, the equilibrium binding constant (K_b) that describes the anti-DAN association with its target hapten (dansyl, DAN) in a biogel is only 5-fold less than the value for anti-DAN dissolved in aqueous buffer ($4.09 \pm 0.10 \times 10^8 \text{ M}^{-1}$ vs $9.04 \pm 0.32 \times 10^7 \text{ M}^{-1}$). Long-term storage experiments on the anti-DAN-doped biogels stored at room temperature show that K_b remains constant for at least 8 months.

Introduction

There has been substantial effort aimed at developing biosensors based on sol–gel-derived xerogels.¹ More recently, researchers have begun to couple the intrinsic power of antibodies (monoclonal and polyclonal) with sol–gel processing chemistry to prepare advanced biogels that can be used as immunoprobes.² Previous antibody-based biogel work has focused on demonstrating that antibodies can function within a xerogel or developing simple immunoprobes based on antibodies sequestered within a xerogel. To date, there have not been any reports on (1) the thermodynamic binding constant that describes the binding between an antibody and an antigen/hapten within a biogel, (2) the effects of biogel storage time on the antibody binding constant, or (3) the mobility of an antibody within an aged biogel.

In this paper we report on the equilibrium binding affinity (K_b) and rotational reorientation dynamics of intact polyclonal anti-dansyl antibodies from rabbit (anti-DAN) that have been sequestered within a sol–gel-derived biogel. This particular system was chosen for several reasons. First, dansyl (DAN) serves simul-

taneously as a hapten and as a fluorescent probe molecule. Second, DAN is solvatochromic so subtle changes in the physicochemical properties within its immediate environment (i.e., within the hapten–antibody combining site on anti-DAN) are readily registered as shifts in the DAN excitation and emission spectra, and/or its excited-state intensity decay kinetics.³ Third, there is a substantial body of literature on the anti-DAN/DAN thermodynamics and rotational reorientation dynamics in aqueous buffer solution.³

Experimental Section

Reagents and Materials. Tetraethylorthosilane (TEOS) was purchased from United Chemical Technologies. Molecular Probes was the source of the polyclonal anti-DAN antibodies. These particular antibodies were produced in rabbit and we used the intact immunoglobulin G (IgG) fraction for all experiments. Dansyl-L-glycine (DAN), HCl, NaCl, and $\text{Na}_2\text{-HPO}_4$ were from Sigma. $\text{NaH}_2\text{PO}_4 \cdot 2\text{H}_2\text{O}$ was a product from Fisher Scientific. All reagents were used as received and all aqueous solutions were prepared by using doubly distilled, deionized water.

Buffer Solutions. All aqueous solutions were prepared in pH 7.4 (0.05 M) phosphate buffer that contained 0.015 M NaCl. Throughout the remainder of this paper, we term this the “buffer”.

Sol–Gel-Derived Biogel Monolith Preparation. A typical stock sol–gel processing solution was prepared by mixing 4.5 mL of neat TEOS, 1.4 mL of H_2O , and 100 mL of 0.1 M HCl in a clean glass vial. After 4 h of mixing, a visually clear

* Author to whom all correspondence should be directed. Phone: 716-645-6800 ext 2162. Fax: 716-645-6963. E-mail: chefvb@acsu.buffalo.edu.

(1) (a) Dave, B. C.; Dunn, B.; Valentine, J. S.; Zink, J. I. *Anal. Chem.* **1994**, *66*, 1120A. (b) Lev, O.; Tsionsky, M.; Rabinovich, L.; Glezer, V.; Sampath, S.; Pankratov, I.; Gun, J. *Anal. Chem.* **1995**, *67*, 22A. (c) Avnir, D. *Acc. Chem. Res.* **1995**, *28*, 328. (d) Ingersoll, C. M.; Bright, F. V. *CHEMTECH* **1997**, *27*, 26. (e) Brennan, J. D. *Appl. Spectrosc.* **1999**, *53*, 106A.

(2) (a) Wang, R.; Narang, U.; Prasad, P. N.; Bright, F. V. *Anal. Chem.* **1993**, *65*, 2671. (b) Jordan, J. D.; Dunbar, R. A.; Bright, F. V. *Anal. Chim. Acta* **1996**, *332*, 83. (c) Livage, J.; Roux, C.; DaCosta, J. M.; Desportes, I.; Quinson, J. F. *J. Sol-Gel Sci. Technol.* **1996**, *7*, 45. (d) Bronshtein, A.; Aharonson, N.; Avnir, D.; Turniansky, A.; Alstein, M. *Chem. Mater.* **1997**, *9*, 2632. (e) Shabat, D.; Grynszpan, F.; Saphier, S.; Turniansky, A.; Avnir, D.; Keinan, E. *Chem. Mater.* **1997**, *9*, 2258. (f) Cichna, M.; Markl, P.; Knopp, D.; Niesner, R. *Chem. Mater.* **1997**, *9*, 2640. (g) Wang, J.; Pamidi, P. V. A.; Rogers, K. R. *Anal. Chem.* **1998**, *70*, 1171. (h) Lan, E. H.; Dunn, B.; Zink, J. I. *Chem. Mater.* **2000**, submitted for publication.

(3) (a) Parker, C. W.; Yoo, T. J.; Johnson, M. C.; Godt, S. M. *Biochemistry* **1967**, *6*, 3408. (b) Yguerabide, J.; Epstein, H. F.; Stryer, L. *J. Mol. Biol.* **1970**, *51*, 573. (c) Brochon, J.-C.; Wahl, P. *Eur. J. Biochem.* **1972**, *25*, 20. (d) Schlessinger, J.; Steinberg, I. Z.; Pecht, I. *J. Mol. Biol.* **1974**, *87*, 725. (e) Chan, L. M.; Cathou, R. E. *J. Mol. Biol.* **1977**, *112*, 653. (f) Timofeev, V. P.; Dudich, I. V.; Sykulev, Y. K.; Nezhlin, R. S.; Franek, F. *FEBS Lett.* **1979**, *102*, 103. (g) Luedtke, R.; Owen, C. S.; Karush, F. *Biochemistry* **1980**, *19*, 1182. (h) Hanson, D. C.; Yguerabide, J.; Schumaker, V. N. *Biochemistry* **1981**, *20*, 6842. (i) Oi, V. T.; Vuong, T. M.; Hardy, R.; Reidler, J.; Dangl, J.; Herzenberg, L. A.; Stryer, L. *Nature* **1984**, *307*, 136. (j) Hanson, D. C. *Mol. Immunol.* **1985**, *22*, 245.

solution resulted. To prepare an anti-DAN-doped biogel, we first prepared an anti-DAN "working" solution in buffer by mixing 10–50 μL of the antibody solution as it came from Molecular Probes (15–20 μM in active antibody) with 2–3 mL of buffer. We then added 1.5 mL of the anti-DAN working solution to a 1.5 mL aliquot of the stock sol–gel processing solution in a standard 1 cm^2 cuvette, and we mixed this solution by inverting the cuvette repeatedly. This mixture generally gelled within 5–20 min.

All biogels were aged at room temperature. Prior to analysis, each biogel was washed repeatedly with buffer and the rinse solutions were tested for anti-DAN antibodies. We were unable to detect anti-DAN leaching from our biogels.

Determining the Anti-DAN/DAN K_b . The binding affinity between anti-DAN and DAN was determined by following the increase in the DAN fluorescence within a biogel as described by Parker.⁴ Corrections were carried out for the background fluorescence and for any volume changes. Initially, we performed a series of titrations on 1–4 μM solutions of anti-DAN dissolved in buffer and added aliquots of DAN to generate intensity vs DAN plots. These data were used to construct Scatchard plots⁵ which yielded K_b . For all solution-phase studies, measurements were made 5 min after the DAN was added to the anti-DAN solution.

The sol–gel-derived biogel monoliths were made by placing a monolith within a clean 1 cm^2 quartz fluorescence cuvette that contained buffer and aliquots of DAN were added to the biogel to generate intensity vs DAN plots. We removed free DAN from the biogel by carefully washing the monoliths with buffer until no DAN emission was detected in the wash solution. We also performed a series of control experiments on identically prepared biogels that contained a nonspecific IgG (anti-fluorescein). These control experiments showed that <2% DAN was nonspecifically associated with the biogel matrix. The intensity vs DAN data were used to construct Scatchard plots⁵ which yielded K_b for the anti-DAN within the biogel. All biogel monolith samples were studied 1 h after they were challenged with DAN. Separate time course experiments showed that the anti-DAN-doped biogels reached pseudo-equilibrium within 20 min of our adding the DAN. The fluorescence intensity was stable for several hours, suggesting we were at equilibrium.

Instrumentation. All steady-state fluorescence measurements were performed with an SLM 48000 MHF spectrofluorometer using a Xe arc lamp and single grating monochromators for excitation and emission. The excitation monochromator was set at 350 nm. Excitation and emission band passes were set to 4 and 8 nm, respectively. All spectra were background corrected by using appropriate blanks.

Time-resolved fluorescence anisotropy and intensity decay data were acquired in the frequency domain by using an SLM 48000 MHF multifrequency phase-modulation fluorometer. An argon ion laser (Coherent, model Innova 90-6) operating at 351.1 nm was used as the excitation source. A band-pass filter (Oriel) was placed in the excitation beam path to minimize extraneous plasma tube super-radiance from reaching the emission detector. The fluorescence from the samples was monitored in the typical L-format after passing through a 420 nm long-pass filter (Oriel) and a Glan-Thompson calcite polarizer. The Pockels cell modulator was operated at a 5 MHz base repetition rate. Frequency-domain data were acquired between 5 and 200 MHz at 5 MHz intervals.

For the excited-state intensity decay measurements, we used dilute solutions of Me_2POPOP dissolved in ethanol as the reference lifetime standard ($\tau = 1.45 \text{ ns}$).⁶

Magic-angle polarization conditions were maintained for all excited-state intensity decay measurements to eliminate bias arising from fluorophore rotational reorientation.⁷ No evidence of birefringence was found in these biogels.

All measurements were performed at $20 \pm 0.1 \text{ }^\circ\text{C}$.

Statistics. All experiments were performed on at least three identically prepared samples. Samples were prepared on different days, using different reagent batches. At least 20 discrete multifrequency data sets were acquired for each sample under a given set of experimental conditions. Results are presented as the average of all measurements. Error bars and reported uncertainties denote one standard deviation from the mean value.

Theory

The theory of static and time-resolved fluorescence spectroscopy has been described in detail elsewhere.⁸ In the current work, we use the steady-state fluorescence spectroscopy to give us insights into the local microenvironment surrounding the DAN moiety and to estimate the anti-DAN/DAN K_b .^{3h,4,5} We use frequency-domain fluorescence spectroscopy^{8–11} to determine the DAN fluorophore anisotropy and intensity decay kinetics which provide information on the local microenvironment surrounding the DAN fluorophore and the mobility of the anti-DAN/DAN complex.

The time-resolved fluorescence intensity decay $I(t)$ is generally described by a sum of exponentials:^{8–11}

$$FI(t) = \sum f_i \exp(-t/\tau_i) \quad (1)$$

where f_i is the fractional intensity of the i -th emissive species with apparent excited-state fluorescence lifetime τ_i . In the frequency domain, the sample under study is excited with sinusoidally modulated light and the experimentally measured parameters are the frequency-dependent phase shift ($\Psi(\omega)$) and modulation ($M(\omega)$). These values are compared by nonlinear regression to the values predicted from an assumed decay law, and the parameters of the model adjusted to yield minimal deviations between the data and the prediction. For any time-domain decay law (eq 1), the frequency-domain data are related by the sine and cosine Fourier transforms:

$$S(\omega) = \frac{\int FI(t) \sin \omega t dt}{\int FI(t) dt} \quad (2)$$

$$C(\omega) = \frac{\int FI(t) \cos \omega t dt}{\int FI(t) dt} \quad (3)$$

where ω is the angular modulation frequency ($\omega = 2\pi f$, f = linear modulation frequency). The sine and cosine Fourier transforms are related to the experimentally

(6) Lakowicz, J. R. *Principles of Fluorescence Spectroscopy*; Plenum Press: New York, 1983; p 88.

(7) Spencer, R. D.; Weber, G. *J. Chem. Phys.* **1970**, *52*, 1654.

(8) (a) Lakowicz, J. R. *Principles of Fluorescence Spectroscopy*; Kluwer Academic/Plenum Press: New York, 1999. (b) Demas, J. N. *Excited-State Lifetime Measurements*; Academic Press: New York, 1983.

(9) Lakowicz, J. R.; Gryczynski, I. In *Topics in Fluorescence Spectroscopy*; Lakowicz, J. R., Ed.; Plenum: New York, 1991; Vol. 1, Chapter 5.

(10) Bright, F. V.; Betts, T. A.; Litwiler, K. S. *CRC Crit. Rev. Anal. Chem.* **1990**, *21*, 389–403.

(11) Bright, F. V. *Appl. Spectrosc.* **1995**, *49*, 14A–19A.

(4) Parker, C. W. In *Handbook of Experimental Immunology*; Weir, D. M., Ed.; Blackwell, Oxford Press: London, 1973; Vol. 1, Chapter 14.

(5) (a) VanHolde, K. E. *Physical Biochemistry*; Prentice Hall: Englewood Cliffs, NJ, 1971; pp 51–75. (b) Bohinski, R. C. *Modern Concepts in Biochemistry*, 3rd ed.; Allyn and Bacon: Boston, MA, 1979; pp 151–154. (c) Connors, K. A. *Binding Constants. The Measurement of Molecular Complex Stability*; John Wiley: New York, 1987; pp 21–138.

measured parameters as follows:

$$\Psi(\omega) = \arctan[S(\omega)/C(\omega)] \quad (4)$$

$$M(\omega) = [S(\omega)^2 + C(\omega)^2]^{1/2} \quad (5)$$

The decay terms (α_i and τ_i) are recovered by minimization of the χ^2 function:

$$\chi^2 = \frac{1}{D} \sum \left(\frac{\Psi(\omega) - \Psi_c(\omega)}{\delta\Psi} \right)^2 + \frac{1}{D} \sum \left(\frac{M(\omega) - M_c(\omega)}{\delta M} \right)^2 \quad (6)$$

In this expression D is the number of degrees of freedom, and $\delta\Psi$ and δM represent the uncertainties in the measured phase and modulation, respectively. The “c” subscript denotes the value calculated based on a given model and set of decay terms.

The time-resolved fluorescence anisotropy decay $r(t)$ can be determined by measuring the time dependence of the parallel ($FI_{\parallel}(t)$) and perpendicular ($FI_{\perp}(t)$) components of the fluorescence:

$$r(t) = \frac{(FI_{\parallel}(t) - FI_{\perp}(t))}{(FI_{\parallel}(t) + 2FI_{\perp}(t))} \quad (7)$$

For a simple isotropic rotor $r(t)$ decays with a single rotational reorientation time, ϕ :^{8–11}

$$r(t) = r_0 \exp(-t/\phi) \quad (8)$$

For more complicated systems, $r(t)$ takes the form of a sum of exponentials:

$$r(t) = r_0 \sum \beta_i \exp(-t/\phi_i) \quad (9)$$

where β_i and ϕ_i are the fractional contribution of the total depolarization and the rotational correlation times attributed to reorientational motion, i , respectively.

In the frequency domain, fluorophore rotational reorientation dynamics are determined from frequency-dependent measurements of differential polarized phase angle Δ ($= \theta_{\perp} - \theta_{\parallel}$) and the polarized modulation ratio Λ ($= m_{\parallel}/m_{\perp}$).^{8–11} If the time-dependent intensity decay is given by eq 1, then the decay of the parallel and perpendicular components of the polarized fluorescence are written:

$$FI_{\parallel}(t) = 1/3 [FI(t)(1 + 2r(t))] \quad (10)$$

and

$$FI_{\perp}(t) = 1/3 [FI(t)(1 - r(t))] \quad (11)$$

where $r(t)$ is the fluorescence anisotropy decay. Regardless of the form of the anisotropy decay, Δ and Λ are given by

$$\Delta = \arctan \left[\frac{D_{\parallel}N_{\perp} - D_{\perp}N_{\parallel}}{N_{\parallel}N_{\perp} + D_{\parallel}D_{\perp}} \right] \quad (12)$$

$$\Lambda = \left[\frac{N_{\parallel}^2 + D_{\parallel}^2}{N_{\perp}^2 + D_{\perp}^2} \right]^{1/2} \quad (13)$$

where N_p and D_p represent the polarized components of the sine and cosine Fourier transforms, respectively,

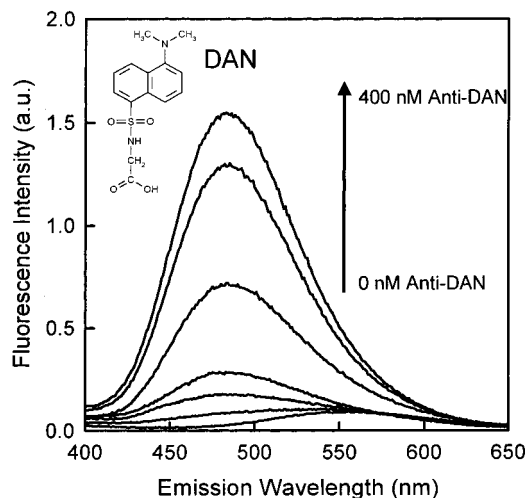


Figure 1. Steady-state DAN emission spectra for 0.2 μM DAN as a function of added anti-DAN between 0 and 400 nM.

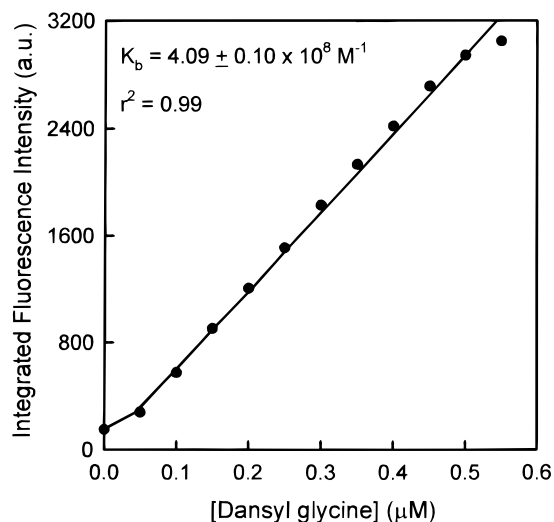


Figure 2. Binding curve between anti-DAN and DAN (dansylglycine). The recovered binding constant is $4.09 \pm 0.10 \times 10^8 \text{ M}^{-1}$.

and the “p” subscript denotes the polarization (\parallel or \perp). The parameters of interest, β_i and ϕ_i , are recovered by fitting the frequency-dependent Δ and Λ data using nonlinear regression methods identical to those used to recover $I(t)$ (vide supra).

Results and Discussion

Steady-State Fluorescence. Figure 1 presents a series of steady-state fluorescence spectra for 0.2 μM DAN (see inset for structure) dissolved in buffer as a function of added anti-DAN (0–400 nM). In the absence of anti-DAN, a weak emission appears at $\sim 550 \text{ nm}$. When anti-DAN is added, the emission shifts blue to $\sim 480 \text{ nm}$ and increases significantly. This is fully consistent with other reports on this system.³ The anti-DAN/DAN K_b can be readily estimated^{3h,4,5} from a plot of the observed fluorescence for a fixed concentration of anti-DAN as a function of added DAN (Figure 2). The recovered K_b from this experiment is $(4.09 \pm 0.10) \times 10^8 \text{ M}^{-1}$. The recovered value is in reasonable agreement with other published results for polyclonal anti-DAN from rabbit complexing with DAN (Table 1).

Figure 3 presents steady-state fluorescence spectra for a pair of 12-week-old anti-DAN-doped biogels after

Table 1. Equilibrium Binding Constants for Polyclonal (IgG fraction from Rabbit) Anti-DAN/DAN Complexation in Various Environments

conditions	K_b (M^{-1})	ref
Aqueous Solutions		
a	$>10^7$	3b
b	$1.4 \pm 0.1 \times 10^8$	3h
c	$4.09 \pm 0.10 \times 10^8$	this work
Biogels ^d		
gel age		
1 week	$9.04 \pm 0.32 \times 10^7$	this work
4 weeks	$8.95 \pm 0.47 \times 10^7$	this work
12 weeks	$9.11 \pm 0.56 \times 10^7$	this work
35 weeks	$9.34 \pm 0.38 \times 10^7$	this work

^a pH 7.4 (0.01 M) phosphate buffer, 0.015 M NaCl, and $T = 23$ °C. ^b pH 7.4 (0.05 M) phosphate buffer, 0.08 M NaCl, $T = 20$ °C. ^c pH 7.4 (0.05 M) phosphate buffer, 0.015 M NaCl, and $T = 20$ °C. ^d Incubation solution surrounding the biogel monoliths is pH 7.4 (0.05 M) phosphate buffer, 0.015 M NaCl, and $T = 20$ °C.

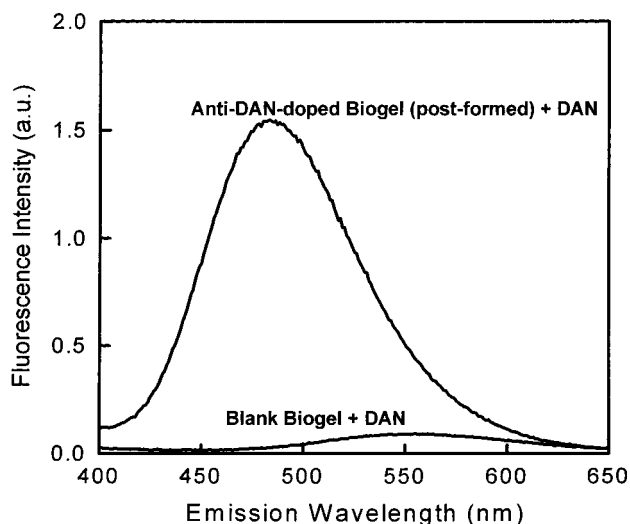


Figure 3. Steady-state emission spectra from a pair of anti-DAN- and nonspecific IgG-doped biogels on being challenged with 0.1 μ M DAN. The biogels contain ~ 0.25 μ M antibody.

they have been incubated in a dilute solution of DAN. The “blank” biogel was prepared by replacing anti-DAN with an equal molar amount of nonspecific IgG. The results of this experiment clearly show that anti-DAN within the biogel can bind to DAN and the observed binding does not result from any significant nonspecific association.

Figure 4 presents steady-state emission spectra for the anti-DAN/DAN complex dissolved in buffer (labeled “buffer”) and compares this spectrum to spectra that are observed when anti-DAN is sequestered within a biogel. Biogel results are shown for two different preparation protocols. In the spectrum labeled “post-formed”, we prepared a biogel as described above and allowed it to age for 8 weeks, immersed it in buffer, made the immersion solution 25 nM in DAN, waited for 1 h, washed the biogel for 2 h with buffer, and then recorded the emission spectrum. The emission maximum from this biogel (483 nm) is in good agreement with the value seen for anti-DAN/DAN dissolved in buffer (485 nm), but it is much different when compared to the emission spectrum for free DAN within a biogel blank ($\lambda_{\max} > 500$ nm). The DAN within the post-formed gel also exhibits some emission in the 400–410 nm region. At

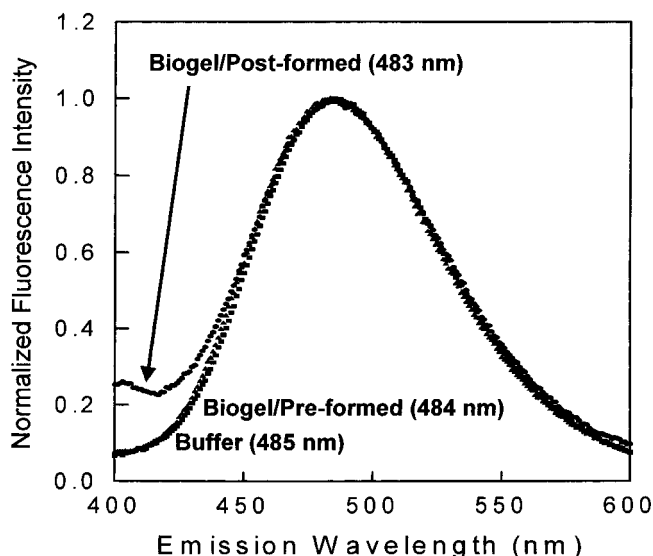


Figure 4. Steady-state emission spectra for anti-DAN/DAN fully complexed in buffer (■), an anti-DAN-doped biogel after challenge with DAN (“postformed”, ●), and an anti-DAN/DAN-doped biogel where the complex was preformed prior to sequestration/encapsulation within a biogel (“preformed”, ▲). The protein concentration is 0.42 μ M in the biogels. For the “postformed” biogel a 0.07 μ M DAN solution was used. For the “preformed” biogel, the molar ratio of DAN:anti-DAN was 0.85.

this time, we are unsure of the origin of this small feature. The second biogel spectrum (labeled “preformed”) was recorded from an 8-week-old biogel that was prepared from the anti-DAN/DAN complex preformed in buffer *prior* to sequestration within the biogel. The emission maximum for this sample (484 nm) is in good agreement with the value seen for anti-DAN/DAN dissolved in buffer (485 nm) and not at all like free DAN within a blank biogel ($\lambda_{\max} > 500$ nm). These steady-state results suggest that the anti-DAN within the biogel selectively complexes with DAN *and* that the hapten/antibody combining site within the anti-DAN antibody is not altered significantly when the antibody is sequestered within a biogel.

Table 1 collects the recovered K_b values for the anti-DAN-doped biogel after the biogels have aged for 1, 4, 12, and 35 weeks and compares these values to the anti-DAN/DAN K_b found in buffer solution. These results illustrate two key points. First, the anti-DAN/DAN K_b decreases by about 5-fold in a biogel relative to the value measured in aqueous buffer. Second, the biogel-doped anti-DAN is remarkably stable, maintaining its affinity for at least 35 weeks.

Time-Resolved Fluorescence. Figure 5 presents typical multifrequency phase-modulation data sets for free DAN (left panel) and anti-DAN/DAN (right panel) dissolved in buffer. The fluorescence intensity decay for free DAN is best described by a double exponential decay law ($\tau_1 = 2.5$ ns and $\tau_2 = 15.9$ ns; $\chi^2_{\text{double}} = 1.05$; $\chi^2_{\text{single}} = 48$). This complex decay profile is a result of a twisted intramolecular charge transfer (TICT) event.¹²

(12) (a) Weber, G. *Biochemistry* **1952**, *51*, 155. (b) Kosower, E. M.; Huppert, D. *Annu. Rev. Phys. Chem.* **1986**, *37*, 127. (c) Nowak, W.; Rettig, W. *J. Mol. Struct. (Theochem.)* **1993**, *283*, 1. (d) Rettig, W.; Lapouyade, R. In *Topics in Fluorescence Spectroscopy*; Lakowicz, J. R., Ed.; Plenum Press: New York, 1994; Vol. 4, Chapter 5, p 109.

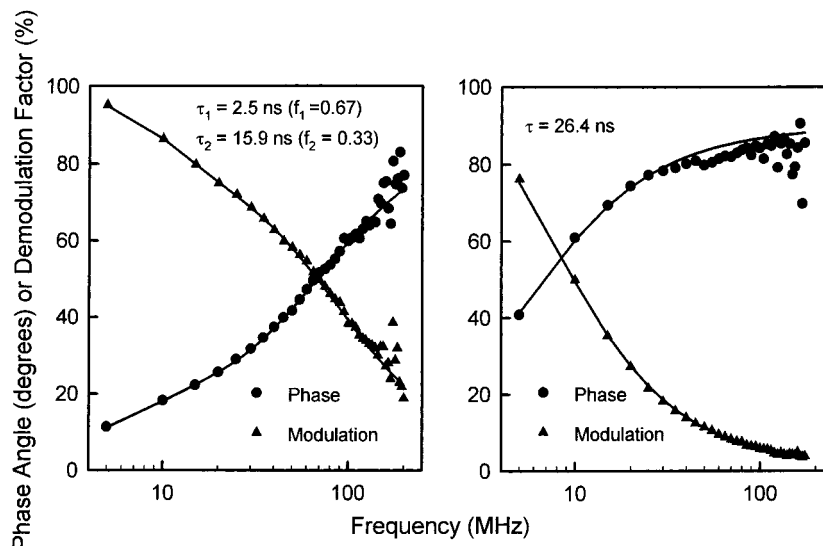


Figure 5. Typical multifrequency phase-modulation data sets (points) and best fits (curves) for free DAN (left panel) and the anti-DAN/DAN complex (right panel) dissolved in buffer.

When the DAN is complexed by anti-DAN, the fluorescence intensity decay is best described a single-exponential decay law ($\tau = 26.4$ ns; $\chi^2 = 1.03$) which is indicative of a TICT shut down.^{3,12} In the anti-DAN-doped biogels at low DAN loadings (to ensure all the DAN is antibody bound), the frequency-domain phase-modulation data (results not shown) are very similar to those shown in the right-hand panel in Figure 5 and the intensity decay kinetics are, at all aging times studied, well-described by a single excited-state fluorescence lifetime of 27 ± 2 ns. This result is fully consistent with our steady-state results and argues that the DAN/anti-DAN combining site within the antibody is not altered appreciably upon anti-DAN sequestration within these biogels.

In a final series of experiments, we set out to explore the rotational mobility of the anti-DAN antibodies within the biogels and to compare these results to the anti-DAN behavior in aqueous buffer. Figure 6 (top panel) presents typical differential polarized phase angle results for free DAN and the anti-DAN/DAN complex when they are dissolved in buffer. The anti-DAN/DAN decay of fluorescence anisotropy is best described ($\chi^2_{\text{single}} = 27.2$ vs $\chi^2_{\text{double}} = 1.13$) by an anisotropic rotor model with two rotational reorientation times ($\phi_1 = 48$ ns and $\phi_2 = 170$ ns). Although the origin of these two rotation reorientation times is a subject of some debate,^{3b,c,e,h-j} our results are completely in line with all previous reports and they are indicative of the intrinsic flexibility and dynamics of an IgG molecule dissolved in buffer. The rotational reorientation dynamics of free DAN itself dissolved in buffer is well-described by a single 0.12 ns rotational reorientation time.

Figure 6 (lower panel) presents differential polarized phase angle results for a 4-week-old, anti-DAN/DAN-doped (post-formed) biogel. These results are characterized by a near zero differential phase angle at all frequencies studied and a high steady-state fluorescence anisotropy ($r = 0.22 \pm 0.01$; limiting anisotropy, $r_0 = 0.24 \pm 0.01$) indicative of limited anti-DAN mobility within the biogel. Given the excited-state lifetime of anti-DAN-bound DAN (~ 27 ns), these results argue that

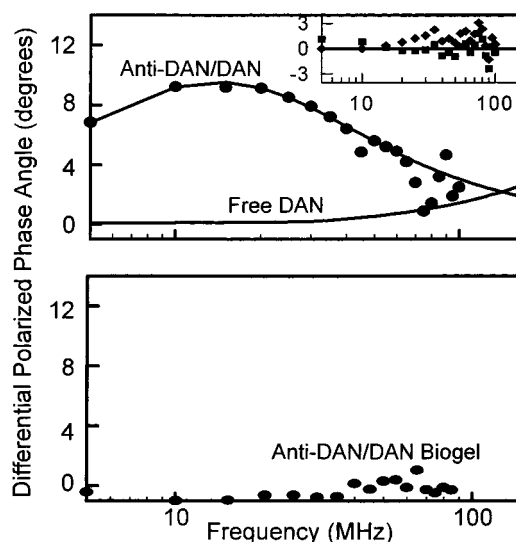


Figure 6. Typical multifrequency differential polarized phase angle data sets (points) and best fits (curves) for free DAN and the anti-DAN/DAN complex. (Top panel) Free DAN (fit only is shown for clarity) and anti-DAN/DAN (data points and fit are shown) each dissolved in buffer. (Lower panel) Anti-DAN/DAN sequestered within a 4-week-old biogel. The protein concentration in these biogels was $0.92 \mu\text{M}$ and a $0.5 \mu\text{M}$ DAN solution was used.

there is no detectable anti-DAN motion within the biogel on a time scale less than 250–270 ns (10τ). This result is interesting given that some globular proteins are reportedly mobile within xerogels,¹³ but other proteins are not.¹⁴ We speculate that the “Y” shape of the anti-DAN IgG may be the underlying origin of its immobility within a biogel.

Conclusions

Intact polyclonal anti-DAN antibodies from rabbit are active within a biogel. The binding affinity that de-

(13) Jordan, J. D.; Dunbar, R. A.; Bright, F. V. *Anal. Chem.* **1995**, *67*, 2436.

(14) Gottfried, D. S.; Kagan, A.; Hoffman, B. M.; Friedman, J. M. *J. Phys. Chem. B* **1999**, *103*, 2803.

scribes the anti-DAN/DAN association decreases 5-fold within the biogel compared to the same system dissolved in aqueous buffer. However, even though the anti-DAN/DAN binding affinity is weakened within the biogel, the binding affinity is nearly 10^8 M^{-1} and the binding within the biogel remains remarkably stable for at least 8 months under ambient storage conditions. Anti-DAN does not exhibit any detectable rotational reorientaion

dynamics within an aged biogel on a time scale between $\sim 100 \text{ ps}$ and $250\text{--}270 \text{ ns}$.

Acknowledgment. This work was generously supported by the National Science Foundation and the Office of Naval Research.

CM990782Z